LAWRENCE
LIVERMORE
NATIONAL
LABORATORY

LLNL-JRNL-496613

Ballistic electron transport in non-equilibrium warm dense gold

T. Ogitsu, Y. Ping, A. Correa, B. Cho, P. Heimann, E. Schwegler, J. Cao, G. Collins

August 30, 2011

High Energy Density Physics

Disclaimer

Ballistic electron transport in non-equilibrium warm dense gold

Tadashi Ogitsu[1], Yuan Ping[1], Alfredo Correa[1], Byoung-ick Cho[2], Phil Heimann[2], Eric Schwegler[1], J. Cao[3] and Gilbert W. Collins[1]
[1]Lawrence Livermore National Laboratory, Livermore, CA 94550
[2]Lawrence Berkeley National Laboratory, Berkeley, CA
[3]Dept. Physics, Florida State University, FL

Abstract

We have measured the time evolution of phase shift at the front and back surfaces of gold nano-foils pumped with 150fs (λ=400nm) pulse laser. The thickness of foils (d~30nm) is roughly one third of the ballistic electron transport range at ambient condition (~100nm). At lower pump fluences, the front and back sides behave similarly, indicating uniform heating by ballistic electrons. As the pump fluence is increased, the phase shift at the front side rises higher than that at the back side, indicating significant reduction of ballistic electron transport range.

Introduction

Advancement on ultrafast pump-probe experimental techniques has enabled investigations on temporal behavior of non-equilibirum Warm Dense Matter (WDM) created by laser pulses[1-10]. A sufficiently short laser pulse (~100fs) is able to excite electrons fast enough so that the absorbed energy does not have a time to dissipate to ionic degree of freedom via electron-phonon coupling[11-17]. In general, electron-electron collision timescale is faster than electron-phonon relaxation timescale, therefore, the electronic degree of freedom reaches to thermal equilibrium before losing its energy to ionic degree of freedom[11, 12]. In other words, the occupation function of quantum mechanical electronic states converged to the Fermi distribution function and the electron temperature is now well defined. Subsequently, electrons cool down via electron-phonon coupling, while ions heat up. This simple description of the dynamics of laser-heated materials is essentially equivalent to the widely-used two-temperature model[18].

Recently, Ultrafast Electron Diffraction measurements were performed on pumped gold nano-foil, and they found that, at a high pump laser fluence, corresponding to the initial electron temperature of a few eV, the evolution of Debye-Waller factor determined from the UED experiments becomes significantly slower than the two-temperature model with the temperature dependent electron-phonon coupling constant[2]. They attributed the slowdown of evolution of DWF to the bond hardening due to the high electron temperature[19-21]. Since the hardened lattice will oscillate with less amplitude for a given lattice temperature. It was later pointed out[22] that, at the high enough electron temperature for the lattice hardening scenario[19-21], the imaginary part of dielectric function, $\varepsilon_2(\omega)$, becomes monotonic, Drude like profile, which is inconsistent with an earlier experimental report on the broadband $\varepsilon_2(\omega)$ measurement of a pumped gold nano-foil[3]. Based on first-principles $\varepsilon_2(\omega)$ simulations, it was suggested that, at such high pump laser fluence, significant amount of electrons might escape from the foil together with sizable amount of kinetic energy, leaving the foil positively charged with a low electron temperature[22]. Although it is speculative, this scenario explains both experimental observations on the time evolution of DWF[2] and $\varepsilon_2(\omega)$[3] consistently. Motivated by this suggestion, a few experimental studies were conducted.

Cho et al. performed the time resolved X-Ray Absorption (XAS) measurements on pumped nano-copper foil and successfully determined the time evolution of electron temperature by fitting to the XAS calculated based on DFT simulations[1]. The time history of electron temperature was well described within the two-temperature model with the electron temperature dependent electron-phonon coupling model[1, 23, 24].

Cao et al. conducted the time resolved electron deflection measurements of pumped copper foil[25], and found that, in fact, significant amount of charge escape from the foil, which rapidly spread out in space due to coulomb repulsion forming a macroscopic size of electron clouds (hundreds of micron meter) in the both side of pumped copper foil (d=30nm), which last for of the order of 100 picoseconds, consistent with the electron escape conjecture[22]. Interestingly, as the pump laser fluence is increased, the electron clouds develop asymmetry between the pumped side and the back side suggesting a development of electron temperature gradient in the foil: an evidence that ballistic transport range of conduction electrons[13-17, 26] be reduced significantly[27] when the fluence of the pump laser reaches to 0.3 J/cm^2.

Motivated by these work, we have conducted series of Fourier Domain Interferometry (FDI) measurements on the both sides of pumped gold foils (d=32nm), and found the strong evidence that the ballistic transport range (~100nm for Au at ambient conditions), decreases significantly at laser intensities an order of magnitude above the damage threshold[13].

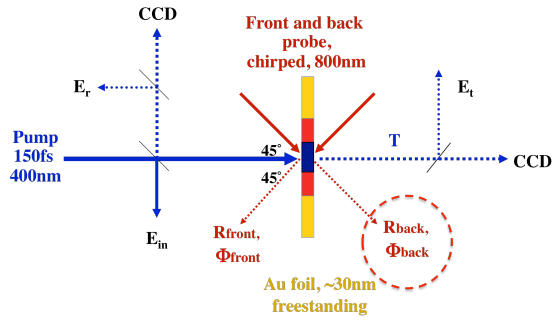

Figure 1: Experimental schematic.

Method

The experimental schematic is shown in Fig. 1. Similar to the setup used in previous experiments, a free-standing Au foil was heated by a 150fs, 400nm laser pulse (pump). The energy deposition of the pump was monitored by three photo-diodes which measure the incident, reflected and transmitted energies. A chirped 800nm probe was incident at 45° onto the target at the pump side. Its reflectivity and phase shift were measured by chirped Fourier Domain interferometry (FDI)[28]. The chirping in the probe enabled single-shot measurements of the time history up to ~50ps. In order to simultaneously probe the other side of the target, the probe pulse was split and the second part was directed onto the back side. The incident angle of the back probe was ~45.5°, slightly different from the front side to avoid interference with the transmitted front probe. The 0.5° difference in the incident angles is negligible in data analysis.

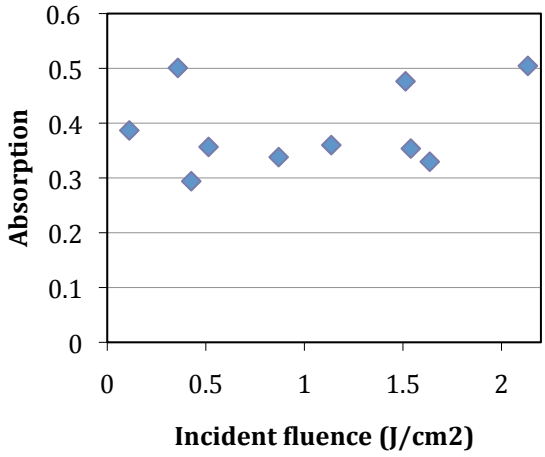

Figure 2: Absorption as a function of incident fluence for Au foils with 400nm pump.

For each shot, the absorbed energy was determined from the reflection and transmission measurements of the pump energy. The absorption as a function of the incident pump fluence is plotted in Fig. 2. It turns out that the absorption is nearly constant at ~40% in the range of our measurements, consistent with previous measurements. The high absorption is a result of interband transition as the pump photon energy ($h\omega$=3.1eV) is above the transition peak at about 3eV[29-31].

Results and discussion

In Figure 3, the phase shift and reflectivity data are presented for three absorbed pump fluences: 0.04, 0.13, and 0.54 J/cm^2. The probe was chirped to ~60ps, resulting in a temporal resolution of ~2.5ps[28]. In all cases, the phase shift rises quickly right after the pumping, then slowly decreases over time. The plateau observed in previous experiments is not pronounced due to limited resolution using the chirped probe. At 0.04 J/cm^2, the font and back data display very similar behavior in both phase shift and the reflectivity, confirming uniforming heating at this fluence. The penetration depth of 400nm photons in

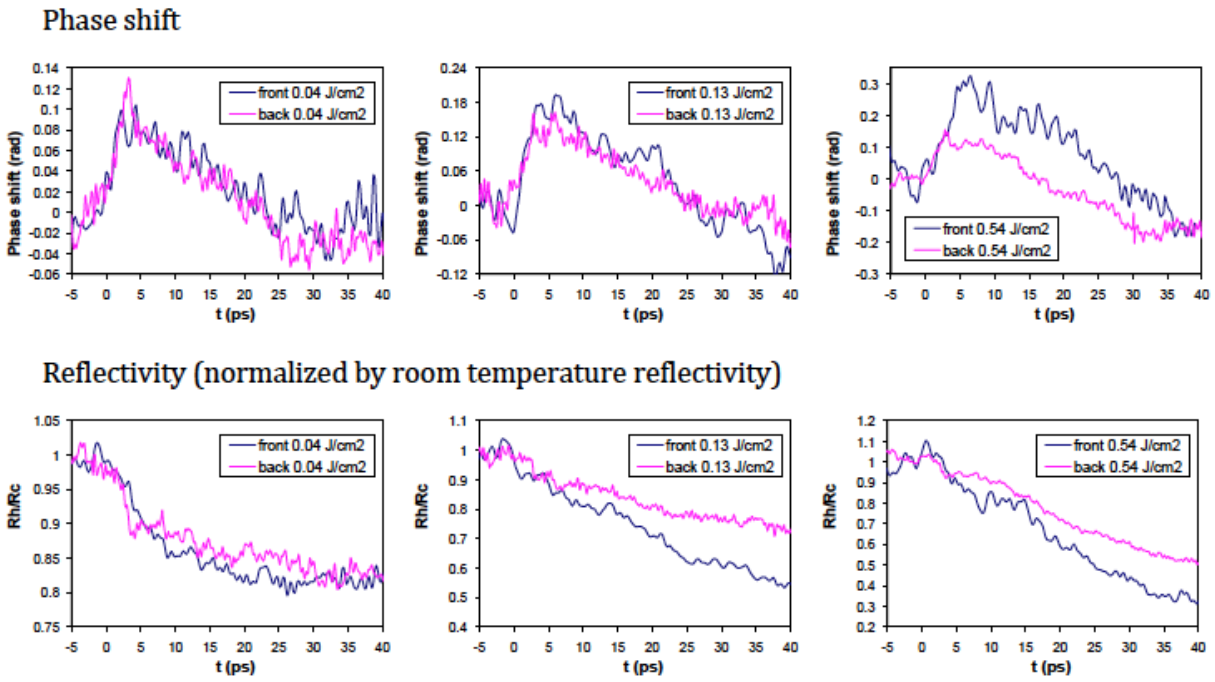

Figure 3: Time history of phase shift and reflectivity measured at front and back sides of gold foil (d=32nm) at three absorbed pump fluences.

Au is only ~10nm. The uniform heating of a 32nm foil is achieved by ballistic transport of excited electrons. As the absorbed fluence increases to 0.13 J/cm^2, difference starts to show up between front and back data. At the highest absorbed fluence of 0.54 J/cm^2, the difference becomes significant. The front phase shift reaches 0.3rad, whileas the maximum of the back phase shift stays at ~0.1rad as in the case of 0.13 J/cm^2. The decreasing rate of the front phase shift is also larger than that at the back side. The difference between the front and the back data indicates development of gradient in the heated foil.

The phase shift data are regrouped in Fig. 4(a) and (b) to show the trend as the absorbed fluence increases. At the front side, both the maximum phase shift and the slope at later time increases with the absorbed fluence. The back side data shows a saturation in the maximum phase shift, and the slope also increases although not as significantly as the front data. The phase shift depends on both the dielectric function and the surface motion. The initial sharp rise of the phase shift is possibly caused by change in the dielectric property due to heating and/or the formation of electron cloud. At later time (>10ps), the phase shift could be dominated by surface motion. Under this assumption, the expansion velocity could be estimated from the slope of the phase shift. The results are shown in Fig. 4(c). The velocity varies from 0.5 to 1.8nm/ps at front and from 0.5 to 1.2nm/ps as the absorbed fluence increases from 0.04 to 0.54 J/cm^2. Further experimental and theoretical investigations are needed to clarify the details of the target expansion. Nevertheless, the observed asymmetry in front and back of heated Au foils is consistent with electron deflection measurements by Cao et al, suggesting that ballistic transport range of conduction electrons in those systems is reduced probably by collisions among the high density of excited electrons (and perhaps holes), which created the gradient of electron temperature between front and back.

Chang et al. performed the optical third harmonics (TH) measurement on pumped silver foils, and analyzed their data using TTM where the reduction of electronic heat conductivity due to presence of *d*-holes was considered[27]. The comparison on the melt depth at t=25ps based on the model calculations and the experimental data show better agreement when the reduction of electronic heat conduction due to *d*-hole is taken into account. They argue that the contribution from ballistic electron transport on thermal conductivity is negligible since "this effect is largely suppressed in our case since both *e-p* and *e-e* scattering rates increases by an order of magnitude when *d* electrons

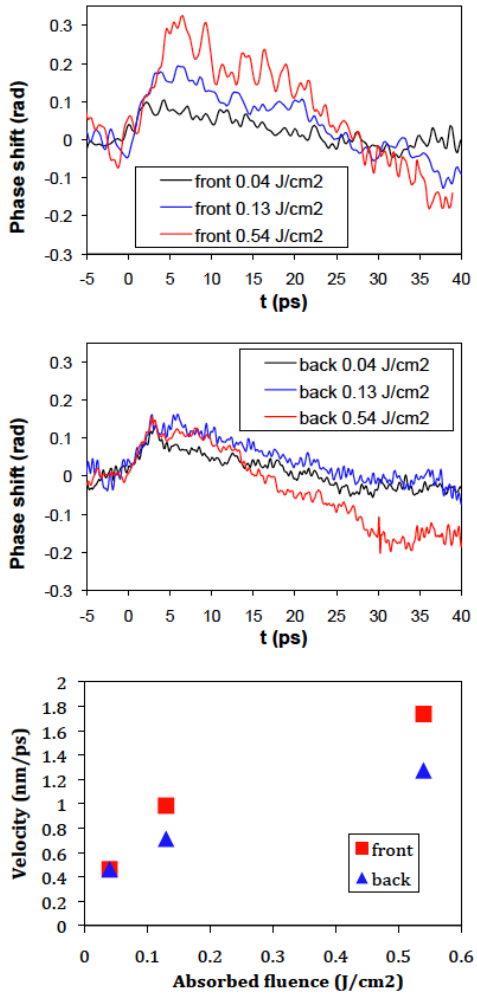

Figure 2: Surface velocity calculated from the phase shift

are exited. This significantly lowers the mean-free path of the electrons."

It is known that the mean free path of excited electron shows monotonic decrease as a function of excitation energy for the range of excitation energy below a few tenth of eV[32-35]. A longer lifetime of *d*-hole than the excitation within *sp*-band (or one that is estimated based on the Fermi liquid theory) was originally reported based on the time resolved two-photon photoemission experiments[36], and supported by subsequent experimental and theoretical studies[37, 38]. All of above point that depression of electron transport for higher excitation energy, and particularly with the presence of *d*-hole, and for diffuse electron transport regime. However, those are not a direct evidence of reduced ballistic range taking place at much shorter time scale, probably except for the escape length measurement[32]. For example, Chang et al.s measurements were at delay time of t=25ps, which is apparently dictated by diffuse transport. Our approach, front/back ultrafast phase shift measurements on pumped nano-foils provide a novel way to determine the ballistic electron transport range in various materials as a function of excitation energy.

Conclusion

We have performed FDI experiments on both front and back side of pumped gold nano-foils (d=32nm). The time evolution of phase shift estimated from the FDI results show clear difference between the pumped side and the back side at high absorbed laser fluence (>0.2 J/cm^2), indicating the reduction of ballistic range by a factor of ~3 from that at ambient condition. This observation is consistent with the time resolved electron deflection measurements on pumped copper nano-foil performed by Cao et al, where asymmetric development of electron could between front and back sides of the target was clearly seen at high pump laser fluence. These methods could be used to determine the ballistic transport range of electrons in various materials at excitation energy on the order of 1-10 eV/atom.

Acknowledgment

We thank C. Cadwalader for target fabrication. This work was performed under the auspices of the U.S Department of Energy Contract No. DE-AC52-07NA27344¤×ÊÔÈ¤, , . ,.

References

1. B.I. Cho, K. Engelhorn, A.A. Correa, T. Ogitsu, C.P. Weber, H.J. Lee, J. Feng, P.A. Ni, Y. Ping, A.J. Nelson, D. Prendergast, R.W. Lee, R.W. Falcone, P.A. Heimann, Phys Rev Lett 106 (2011) 167601.
2. R. Ernstorfer, M. Harb, C.T. Hebeisen, G. Sciaini, T. Dartigalongue, R.J.D. Miller, Science 323 (2009) 1033.
3. Y. Ping, D. Hanson, I. Koslow, T. Ogitsu, D. Prendergast, E. Schwegler, G. Collins, A. Ng, Phys Rev Lett 96 (2006)
4. T. Ao, Y. Ping, K. Widmann, D.F. Price, E. Lee, H. Tam, P.T. Springer, A. Ng, Phys Rev Lett 96 (2006) 055001.
5. A. Ng, T. Ao, F. Perrot, M.W.C. Dharma-Wardana, M.E. Foord, Laser and Particle Beams 23 (2005) 527.
6. K. Widmann, T. Ao, M.E. Foord, D.F. Price, A.D. Ellis, P.T. Springer, A. Ng, Phys Rev Lett 92 (2004) 125002.
7. R.W. Lee, S.J. Moon, H.-K. Chung, W. Rozmus, H.A. Baldis, G. Gregori, R.C. Cauble, O.L. Landen, J.S. Wark, A. Ng, S.J. Rose, C.L. Lewis, D. Riley, J.-C. Gauthier, P. Audebert, J. Opt. Soc. Am. B 20 (2003) 770.

8. G. Dyer, R. Sheppherd, J. Kuba, E. Fill, A. Wootton, P. Patel, D. Price, T. Ditmire, Journal of Modern Optics 50 (2003) 2495.
9. Y. Ping, D. Hanson, I. Koslow, T. Ogitsu, D. Prendergast, E. Schwegler, G. Collins, A. Ng, Physics of Plasmas 15 (2008) 056303.
10. G.M. Dyer, A.C. Bernstein, B.I. Cho, J. Osterholz, W. Grigsby, A. Dalton, R. Shepherd, Y. Ping, H. Chen, K. Widmann, T. Ditmire, Phys Rev Lett 101 (2008) 015002.
11. W.S. Fann, R. Storz, H.W.K. Tom, J. Bokor, Phys Rev B 46 (1992) 13592.
12. W.S. Fann, R. Storz, H.W.K. Tom, J. Bokor, Phys Rev Lett 68 (1992) 2834.
13. J. Hohlfeld, S.S. Wellershoff, J. G¸dde, U. Conrad, V. J‰hnke, E. Matthias, Chemical Physics 251 (2000) 237.
14. M. Bonn, D.N. Denzler, S. Funk, M. Wolf, S.S. Wellershoff, J. Hohlfeld, Phys Rev B 61 (2000) 1101.
15. J. Hohlfeld, J.G. Müller, S.S. Wellershoff, E. Matthias, Applied Physics B: Lasers and Optics 64 (1997) 387.
16. C. Suarez, W.E. Bron, T. Juhasz, Phys Rev Lett 75 (1995) 4536.
17. T. Juhasz, H.E. Elsayed-Ali, G.O. Smith, Su, aacute, C. rez, W.E. Bron, Phys Rev B 48 (1993) 15488.
18. S.I. Anisimov, Kapeliov.Bl, T.L. Perelman, Zhurnal Eksperimentalnoi I Teoreticheskoi Fiziki 66 (1974) 776.
19. F. Bottin, ccedil, ois, eacute, G. rah, Phys Rev B 75 (2007) 174114.
20. S. Mazevet, Cl, eacute, J. rouin, V. Recoules, P.M. Anglade, G. Zerah, Phys Rev Lett 95 (2005) 085002.
21. V. Recoules, Cl, eacute, J. rouin, G. rah, P.M. Anglade, S. Mazevet, Phys Rev Lett 96 (2006) 055503.
22. Y. Ping, A.A. Correa, T. Ogitsu, E. Draeger, E. Schwegler, T. Ao, K. Widmann, D.F. Price, E. Lee, H. Tam, P.T. Springer, D. Hanson, I. Koslow, D. Prendergast, G. Collins, A. Ng, High Energy Density Physics 6 (2010) 246.
23. Z. Lin, L.V. Zhigilei, V. Celli, Phys Rev B 77 (2008)
24. P.B. Allen, Phys Rev B 36 (1987) 2920.
25. J. Cao, to be published
26. S.D. Brorson, J.G. Fujimoto, E.P. Ippen, Phys Rev Lett 59 (1987) 1962.
27. W.L. Chan, R.S. Averback, D.G. Cahill, A. Lagoutchev, Phys Rev B 78 (2008) 214107.
28. S. Rebibo, J.P. Geindre, P. Audebert, G. Grillon, J.P. Chambaret, J.C. Gauthier, Laser and Particle Beams 19 (2001) 67.
29. D. Beaglehole, Proceedings of the Physical Society 85 (1965) 1007.
30. J.N. Hodgson, Journal of Physics and Chemistry of Solids 29 (1968) 2175.
31. P.B. Johnson, R.W. Christy, Phys Rev B 6 (1972) 4370.
32. I. Lindau, W.E. Spicer, Journal of Electron Spectroscopy and Related Phenomena 3 (1974) 409.
33. C.J. Tung, J.C. Ashley, R.H. Ritchie, Surface Science 81 (1979) 427.
34. J.C. Ashley, C.J. Tung, R.H. Ritchie, Surface Science 81 (1979) 409.
35. A.F. Mayadas, Journal of Applied Physics 39 (1968) 4241.
36. E. Knoesel, A. Hotzel, M. Wolf, Phys Rev B 57 (1998) 12812.
37. V.P. Zhukov, E.V. Chulkov, P.M. Echenique, Phys Rev B 68 (2003) 045102.
38. A. Gerlach, K. Berge, A. Goldmann, I. Campillo, A. Rubio, J.M. Pitarke, P.M. Echenique, Phys Rev B 64 (2001) 085423.